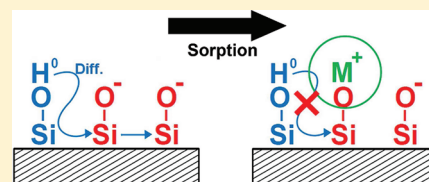


# Probing the Surface Structure of Divalent Transition Metals Using Surface Specific Solid-State NMR Spectroscopy

Harris E. Mason,<sup>\*,†</sup> Stephen J. Harley,<sup>†</sup> Robert S. Maxwell,<sup>†</sup> and Susan A. Carroll<sup>†</sup>

<sup>†</sup>Physical and Life Sciences Directorate, Lawrence Livermore National Laboratory, 7000 East Avenue Livermore, California 94551, United States

**ABSTRACT:** Environmental and geochemical systems containing paramagnetic species could benefit by using nuclear magnetic resonance (NMR) spectroscopy due to the sensitivity of the spectral response to small amounts paramagnetic interactions. In this study, we apply commonly used solid-state NMR spectroscopic methods combined with chemometrics analysis to probe sorption behavior of the paramagnetic cations  $\text{Cu}^{2+}$  and  $\text{Ni}^{2+}$  at the amorphous silica surface. We exploit the unique properties of paramagnets to derive meaningful structural information in these systems at low, environmentally relevant cation surface loadings by comparing the NMR response of sorption samples to paramagnetic free samples. These data suggest that a simple sorption model where the cation sorbs as inner sphere complexes at negatively charged, deprotonated silanol sites is appropriate. These results help constrain sorption models that are used to describe metal fate and transport.



## INTRODUCTION

Models which can accurately predict the fate and transport of subsurface contaminants are an area of intense geochemical research. Extensive work has gone into developing models which can accurately predict the behavior of sorbed cations based solely on measured solution chemistry.<sup>1–6</sup> These models are based on electrostatic interactions between solution species and mineral surfaces and have demonstrated some success in modeling the sorption behavior over a range of solution chemistries. However, these models are often overdefined and therefore need accurate spectroscopic studies to constrain input parameters.

Detailed structural information about the sorbed cation complexes has been gleaned from various spectroscopic investigations of reactions between divalent metals and mineral surfaces. Specifically, we focus on the previous work aimed at the interactions of paramagnetic cations  $\text{Cu}^{2+}$  and  $\text{Ni}^{2+}$  with silicate mineral surfaces. A wealth of information about the sorption of Cu on the amorphous silica surface has been derived from X-ray adsorption (XAS) and electron paramagnetic resonance (EPR) spectroscopic studies.<sup>7–12</sup> These studies find that the Cu binds strongly to the silica surface as inner sphere complexes and that Cu dimers can form at low surface coverages.<sup>9,10</sup> Contrasting EPR results have also suggested that surface sorption is limited and that  $\text{Cu}(\text{OH})_2$  precipitation dominates.<sup>7,8</sup> Similarly, XAS methods have also been applied to the study of Ni interactions with mineral surfaces.<sup>13–16</sup> These studies have suggested that at short reaction times the Ni forms inner sphere complexes but that at longer times the reactions are dominated by the formation of Ni surface precipitates.<sup>13</sup>

The study of Cu and Ni containing systems by NMR spectroscopy presents some unique challenges and opportunities to derive structural information from simple NMR experiments. In the fields of environmental chemistry and

geochemistry the study of systems containing paramagnetic species with NMR spectroscopy has largely been avoided due to the perception that their presence precludes the observation of useful structural information. Therefore, most NMR based sorption studies have focused on loading surfaces with moderately high concentrations of diamagnetic species such as  $\text{Na}^+$ ,  $\text{Cs}^+$ ,  $\text{Al}^{3+}$ , and  $\text{PO}_4^{3-}$  which are easily observed with standard solid-state NMR methods.<sup>17–21</sup> However, strong interactions between NMR observable nuclei and the unpaired electrons present in paramagnetic species have been successfully exploited to derive precise structural information on organometallic complexes.<sup>22,23</sup>

In this study, we exploit what are traditionally considered the detrimental effects of paramagnetic species on the NMR spectral response to derive information about the surface structure of sorbed metal species at low, environmentally pertinent surface loadings. There is a need for methodologies which can differentiate between sorption and precipitation of sparingly soluble actinide species like Pu and Np, which are also paramagnetic.<sup>24</sup> We present the results of NMR spectroscopic investigation of  $\text{Cu}^{2+}$  and  $\text{Ni}^{2+}$  sorption on the amorphous silica surface as paramagnet analogues to these actinide systems. The methods employed here allow us to identify the surface ligand with which these cations interact. It is largely assumed based on electrostatic arguments that these cations should prefer to bind at negatively charged surface sites (i.e.,  $>\text{SiO}^-$ ), but no study has directly investigated this assertion.

**Received:** October 21, 2011

**Revised:** January 25, 2012

**Accepted:** February 9, 2012

**Published:** February 9, 2012

## MATERIALS AND METHODS

**Sorption Experiments.** The  $\text{Cu}^{2+}$  and  $\text{Ni}^{2+}$  sorption experiments were conducted as a function of surface loading at pH 8 and 9, respectively. These pH conditions correspond to their sorption maxima<sup>5</sup> and were maintained through the periodic addition of 0.01 N NaOH by a Metrohm Titrand 902 autotitration unit. To ensure surface equilibration, 0.5 g of high surface area amorphous silica (Mallinckrodt silica: 306 m<sup>2</sup>/g surface by BET, 75–100  $\mu\text{m}$  particle size) was reacted in 100 mL of 0.1 M NaCl solution at the desired pH for 22 h before proceeding with the sorption reaction. After the equilibration step, an aliquot of the cation stock solution (10 mM  $\text{CuCl}_2$  or 1 mM  $\text{NiCl}_2$ ) was added in order to achieve the desired initial concentration (Table 1), and the system was allowed to react

**Table 1. Results of Solution Chemistry Measured for the Sorption Experiments<sup>a</sup>**

sample	pH	$M^{2+}$ <sub>initial</sub> ( $\mu\text{mol}$ )	$M^{2+}$ <sub>final</sub> ( $\mu\text{mol}$ )	% <sub>removed</sub>	bulk coverage (nmol $M^{2+}$ /m <sup>2</sup> $\text{SiO}_2$ )	% coverage
Cu 01	8	1.0	0.012	98.8	6.5	0.33
Cu 1	8	10.0	0.15	98.5	64.4	3.23
Ni 01	9	1.0	0.75	24.6	1.6	0.08
Ni 1	9	10.0	1.73	82.6	54.0	2.71

<sup>a</sup>The % coverage is calculated assuming a surface silanol density of 2  $\mu\text{mol}/\text{m}^2$  (see text).

for 2 h. For NMR analyses, the samples were collected by suction filtration and dried overnight at 60 °C. <sup>1</sup>H NMR data (vide infra) showed that a hydration layer remained on the silica surface following the drying procedure indicating that it did not significantly alter the surface structure. Ten mL aliquots of the reaction solution were collected immediately after the 22 h equilibration period and after the 2 h sorption reaction. These solutions were filtered through a 0.2  $\mu\text{m}$  syringe filter and submitted to ICPMS analysis. The final surface loadings were calculated through difference from the initial and final solution concentrations. Control samples for baseline comparison of the NMR response were produced at pH 8 and 9 by immediately halting the reaction after the equilibration step. The control sample produced at pH 9 was also physically mixed with  $\text{Ni}(\text{OH})_2$  colloids in an agate mortar and pestle in order to test the response to the presence of a separate precipitated phase.

**NMR Spectroscopy.** Solid-state <sup>29</sup>Si single pulse (SP) and <sup>29</sup>Si{<sup>1</sup>H} cross-polarization magic angle spinning (CP/MAS) experiments were conducted on a 300 MHz Tecmag Apollo spectrometer at operating frequencies of 59.63 and 300.19 MHz for <sup>29</sup>Si and <sup>1</sup>H, respectively. The <sup>29</sup>Si{<sup>1</sup>H} CP/MAS spectra were collected with continuous-wave CP excitation over a range of CP contact times at spinning rate of 3 kHz using a Chemagnetics probe configured for 7.5 mm (o.d.) rotors. A 6  $\mu\text{s}$  <sup>1</sup>H excitation pulse was used, and <sup>29</sup>Si was matched on the +1 sideband of kaolinite. All <sup>29</sup>Si spectra were referenced with respect to tetramethylsilane (TMS) using an external kaolinite standard ( $\delta_{\text{Si}} = -92$  ppm). <sup>1</sup>H single pulse (SP) MAS NMR spectra were collected on a 400 MHz Bruker Avance spectrometer at an operating frequency of 400.06 MHz. The samples were contained in 4 mm (o.d) rotor and spun at a 12 kHz spinning rate with a 4 mm Bruker triple resonance probe. Standard inversion recovery techniques were employed to measure <sup>1</sup>H spin–lattice relaxation constants ( $T_1$ ). All <sup>1</sup>H spectra were collected with a 6  $\mu\text{s}$  excitation pulse and are

referenced with respect to an external sample of TMS ( $\delta_{\text{H}} = 0$  ppm). In order to quantify the NMR spectral intensities for all NMR experiments, the samples were loaded in preweighed  $\text{ZrO}_2$  ceramic rotors, and their weights were recorded.

**Chemometrics Analysis of NMR Data.** Chemometric methodologies are a powerful group of techniques that extract relevant spectral information from subtle variations in large multidimensional data sets.<sup>25–27</sup> Here two subsets of chemometrics are utilized: evolving factor analysis (EFA) and multivariate curve resolution (MCR). First EFA<sup>28</sup> is applied to the compiled CP NMR data set whose rows are comprised of a single CP spectrum for a characteristic contact time, and the columns represent the intensity change for a discrete frequency as a function of contact time. The advantage of EFA is that it merely seeks to compile those components who share similar variant behavior into separate factors and is independent of a chemical model. Those factors that show more variance than the variance of the original spectra contain the dynamics of interest. All other factors were discarded. Then these kept factors are fed into a multivariate curve resolution method utilizing an alternating least-squares algorithm (MCR-ALS) to iteratively deconvolute the spectroscopic data matrix (**D**) into a pure component (**C**) and pure spectra (**S<sup>T</sup>**) profile according to

$$\mathbf{D} = \mathbf{CS}^T + \mathbf{E} \quad (1)$$

**E** is the residual matrix and contains the variance unexplained by **CS<sup>T</sup>**; here it is assumed to be independent and have constant variance. The subtleties of this technique are explained thoroughly in the literature.<sup>29,30</sup> This so-called soft-model (or model-free) approach is advantageous when a hard-model is unavailable or inadequately describes the spectral response.

## RESULTS AND DISCUSSION

**Identification of Ligand Adsorption Sites.** At face value, the individual <sup>29</sup>Si{<sup>1</sup>H} CP/MAS spectra of the sorption samples do not appear much different from the control samples (Figure 1). They all have the same three major peaks present at

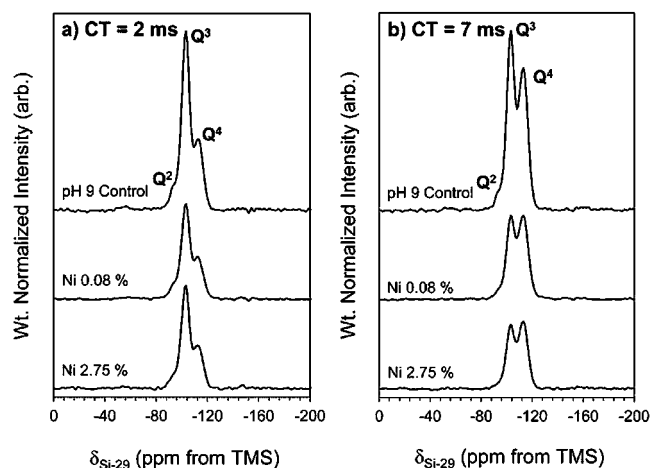


**Figure 1.** <sup>29</sup>Si{<sup>1</sup>H} CP/MAS spectra collected contact time of 2 ms (left) and 7 ms (right) for the pH 9 control sample and two Ni sorption samples.

−93.4, −103.1, and −113.2 ppm which are typically assigned to the Q<sup>2</sup>, Q<sup>3</sup>, and Q<sup>4</sup> silica sites. The Q<sup>n</sup> notation refers to the number of bridging oxygens shared with surrounding silica tetrahedra with the Q<sup>2</sup> and Q<sup>3</sup> sites representing silanol sites

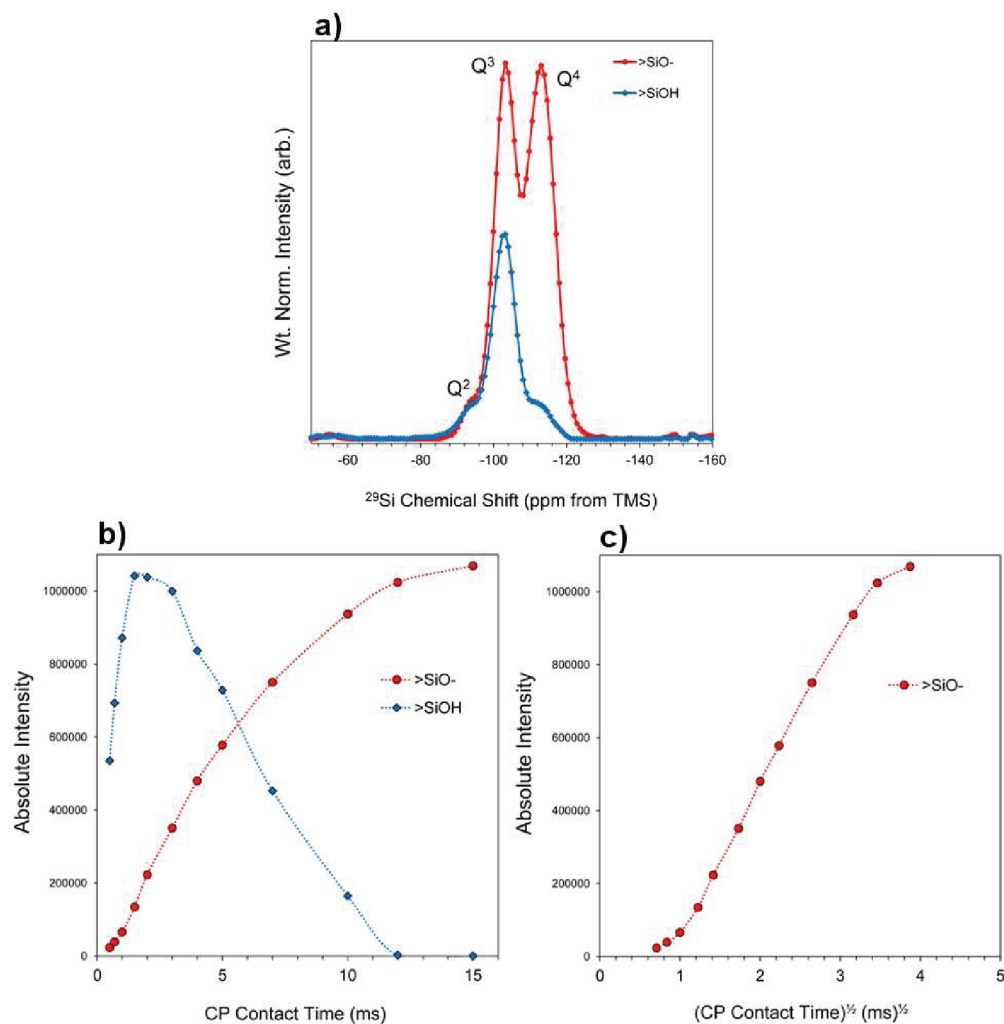


**Figure 2.** Results of chemometrics analysis for the pH 9 control sample. **a)** The two components which fully describe the intensity variation. **b)** The intensity versus contact time profiles for the  $>\text{SiO}^-$  and  $>\text{SiOH}$  components. **c)** The intensity profile of the  $>\text{SiO}^-$ . The dotted lines are present only to guide the eye.

whose remaining oxygens are terminated with silanol protons and the  $\text{Q}^4$  site representing fully coordinated internal siloxane groups.<sup>17,31</sup> Since the  $^1\text{H}$  exists only on the surface, these spectra are surface selective and represent the species on or directly associated with the silica surface. Although the presence of paramagnetic cations does not change observed peak chemical shifts or widths in the sorption samples, there are large decreases in the integrated spectral intensities of these peaks (Figure 1). Unlike the results from  $^{29}\text{Si}$  SP/MAS NMR, the peak intensities in individual  $^{29}\text{Si}\{^1\text{H}\}$  CP/MAS spectra are not representative of the relative abundances of the silica species.<sup>32</sup> Therefore, we must consider how the intensity of these peaks varies as a function of the CP contact time to quantify the effects the paramagnetic species have in these systems.

We have applied chemometrics analysis to the variable contact time  $^{29}\text{Si}\{^1\text{H}\}$  CP/MAS spectra and have identified two unique spectral components whose presence we attribute to the existence of protonated (Figure 2a, blue) and deprotonated (Figure 2a, red) silica surface sites. We see that the two spectral components contain contributions from all three silica sites but have very different intensity profiles (Figure 2b). The lesser of the two components has an intensity profile which grows in rapidly with an average  $T_{\text{SiH}}$  of 1.0 ms and decays away with an

average  $T_{1\rho,\text{H}}$  of 3 ms. This behavior is characteristic of silica sites which are directly bound to protons,<sup>31,32</sup> and we assign this component to protonated surface silanols ( $>\text{SiOH}$ ). The other site, however, exhibits the opposite behavior with its intensity growing in more slowly and with no observed  $T_{1\rho,\text{H}}$  decay. If the intensity of this second site is instead plotted as a function of the square root of the contact time, then there is a clear linear region in the middle of the profile (Figure 2). This observed behavior is characteristic of a diffusion limited process.<sup>33</sup> In our system, this process is not a physical diffusion but rather a diffusion of magnetization energy which we will refer to as spin or magnetization diffusion.<sup>34</sup> We assign this component to deprotonated silica species, because they are spatially distinct from protons and are observed in the CP/MAS spectra only by long-range couplings through spin diffusion. This assignment is further corroborated by the large presence of the  $\text{Q}^4$  siloxane groups in this component which are by definition deprotonated and are present due to long-range couplings (Figure 2a, red). The  $\text{Q}^2$  and  $\text{Q}^3$  sites contained in this fraction we assign to deprotonated surface silanol groups ( $>\text{SiO}^-$ ). We attribute the contribution of the  $\text{Q}^4$  sites to direct coordination or close proximity ( $<5$  Å) to the protonated surface silanol groups. Since these  $\text{Q}^4$  are contained within the bulk silica and unlikely to be important in the

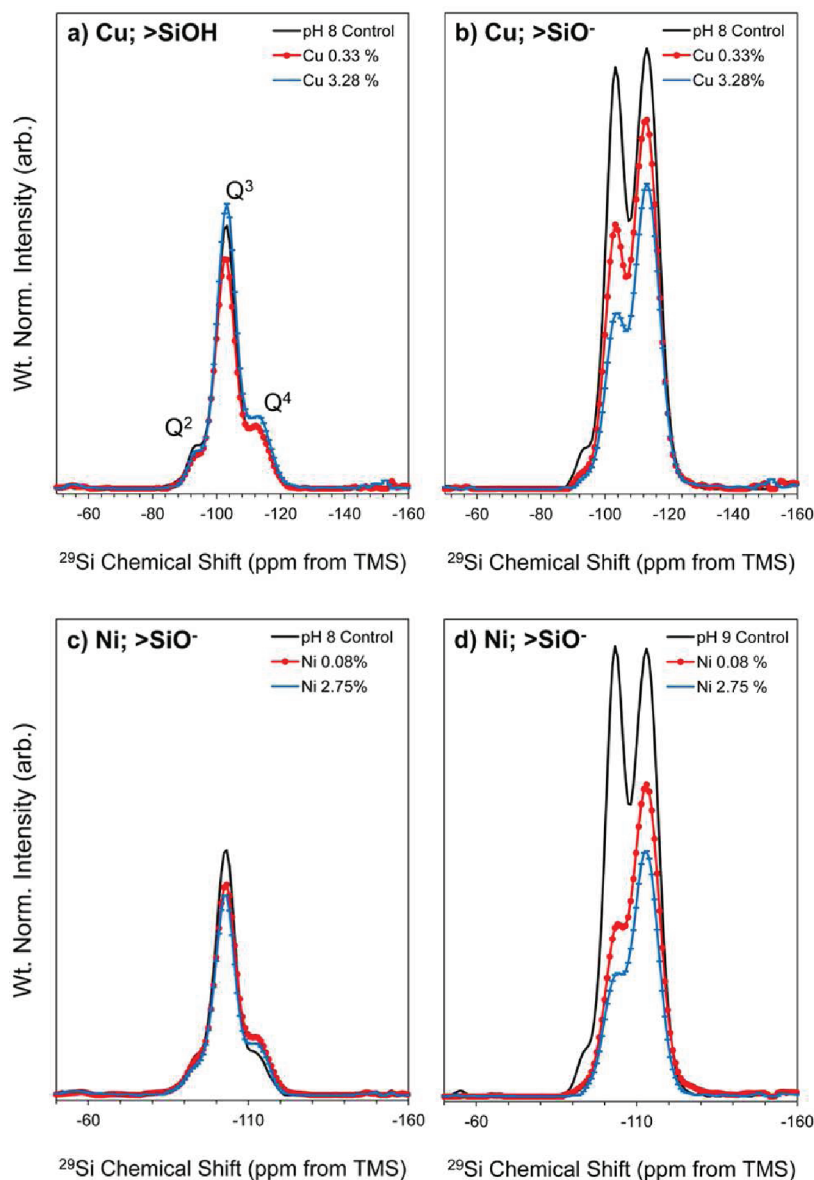


**Figure 3.** The results of chemometrics analysis for the a – b) Cu and c – d) Ni sorption samples compared to that obtained for their respective control samples. All spectra were collected for the same number of acquisitions (4096), and their intensities are scaled based on their measured weights.

sorption process, they will not be discussed further. All other discussion will center on the Q<sup>2</sup> and Q<sup>3</sup> silanol surface sites.

With the assignment of these components to >SiOH and >SiO<sup>-</sup> surface groups we can begin to draw conclusions about the sorption of Cu<sup>2+</sup> and Ni<sup>2+</sup> to the silica surface. We find that changes in the integrated CP signal intensity can be attributed to the sorption of Ni and Cu metals occurs as inner sphere complexes at >SiO<sup>-</sup> surface sites (Figures 3 and 4). When we compare the weight normalized spectral components of the sorption samples to those of the control samples, we observe only slight changes in signal intensity for the protonated fraction (which are within experimental error) but major changes in the deprotonated fraction. Assuming a conservative surface silanol density of 2  $\mu\text{mol}/\text{m}^2$  for amorphous silica at pH 8/9,<sup>17</sup> and the amount of Cu and Ni uptake, then surface site coverage ranges from about 0.1 to 3% (Table 1). For both the Cu and Ni samples, we observe large systematic decreases in the signal intensity of the >SiO<sup>-</sup> component as a function of

surface loading. For the Cu samples, the intensity of the Q<sup>3</sup> peaks relative to those of the control reduces by 37.6% for the lowest concentration sample (0.33% surface coverage) and 56.6% for the highest concentration (3.23% surface coverage). For the Ni samples, these same peaks reduce by 62.5% for the low concentration sample (0.08% surface coverage) and 70.9% for the high concentration sample (2.7% coverage). If the intensity losses were the result of site blockage alone, then we should expect these to be proportional to the surface coverage. However, we note the largest decreases in the Ni system where the coverage is lowest. We attribute the larger decreases to the more paramagnetic character of the Ni<sup>2+</sup> cation which as two unpaired electrons compared to the single unpaired electron in the Cu<sup>2+</sup> cation. The observed effects appear to result only through the interactions with the silica surface with paramagnetic species.

We clearly observe a systematic effect in the CP/MAS data as we increase the concentration of paramagnetic species, but we

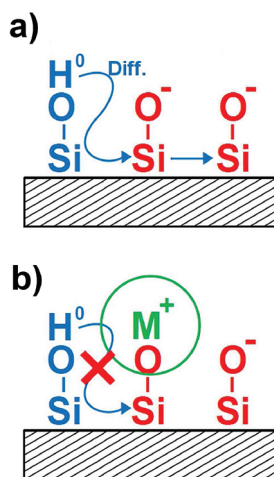


**Figure 4.** Schematic representations of  $^1\text{H}$  magnetization transfer (blue arrows) through spin diffusion between different surface silica sites. a) In the absence of paramagnetic cations magnetization is shuttled from the  $>\text{SiOH}^0$  (blue) to the  $>\text{SiO}^-$  groups (red). b) The presence of a  $>\text{SiOM}^+$  (red and green) surface species blocks the magnetization transfer due to the presence of unpaired electrons (represented by the green circle).

need to test if these effects result only from through bond interactions with the surface, or if they would also occur if a distinct precipitated phase is present. When we analyze the data collected for the pH 9 control sample and the physical mixture of  $\text{Ni}(\text{OH})_2$  colloids (not shown), we observe no differences between the observed intensities and that of the pristine pH 9 control sample. The absence of an effect in this sample supports our interpretation that intensity changes result from bonding interactions between the sorbed metal species and the  $>\text{SiO}^-$  groups on the amorphous silica surface. This result does not preclude the presence of a precipitated phase in our sorption samples but indicates that if such a phase is present that it does not affect the observed NMR signal. Therefore, we propose that in the absence of sorbed paramagnets,  $^1\text{H}$  magnetization diffusion is efficient between the  $>\text{SiOH}$  and  $>\text{SiO}^-$  groups (Figure 4a). In the presence of the sorbed paramagnetic species this diffusion is inhibited due to the unpaired electron density interacting more strongly with the  $>\text{SiO}^-$  than with surrounding  $^1\text{H}$  (Figure 4b) causing the characteristic decrease in signal intensity we observe with increasing sorbent concentration. These data also suggest that the transition between sorption and precipitation could be identified with NMR spectroscopy of samples made with progressively increasing surface loadings. The transition from sorption to precipitation would be marked by a continued increase in metal uptake as measured by solution chemistry but no additional reduction in the NMR intensities.

All the above structural observations are only possible because of spectral interferences from paramagnetic species. Similar to the above  $\text{Ni}(\text{OH})_2$  colloid experiment, the absence or decrease in the EPR spectral response in Cu uptake experiments has been used as evidence for either the precipitation of  $\text{Cu}(\text{OH})_2$  or the formation of diameric Cu-hydroxide species.<sup>7,8,12</sup> The understanding is that these phases lose the paramagnetic character of the  $\text{Cu}^{2+}$  and will not cause a response in the EPR experiment. Therefore, the presence of such a phase in our samples would be equally ineffective at producing the NMR responses we observe. The large spectral

response observed for our highest Cu loadings suggests that none of the previously suggested Cu-hydroxide phases have formed in our experiments.

**Identification of External versus Internal Sorption Sites.** Powerful information about the bonding environment of these cations can also be gleaned by directly observing  $^1\text{H}$  in a  $^1\text{H}$  SP/MAS NMR experiment (Figure 5). These results

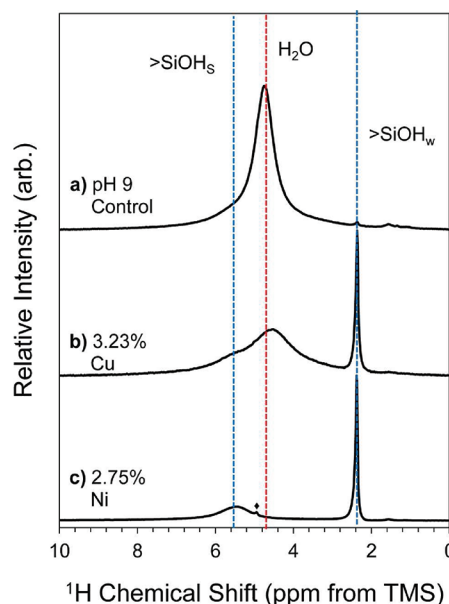


**Figure 5.** Sample  $^1\text{H}$  NMR spectra collected for the a) pH 9 control sample, and the highest loaded b) Cu and c) Ni samples.  $\blacklozenge$  marks the location of a spectral artifact.

indicate that the surface sorbed metal species strongly interact with surface water species but interact less strongly with  $>\text{SiOH}$ . This is evidenced by again comparing the NMR signal obtained for control samples to that of the samples containing surface sorbed metals. What is immediately apparent is the suppression of the 4.7 ppm peak corresponding to water sorbed to the dried silica surface from the spectra of the sorption samples (Figure 5). Also observed is the conspicuous emergence of a strong, sharp (0.1 ppm fwhm)  $^1\text{H}$  peak near 2 ppm from isolated, weakly H-bonded  $\text{SiOH}$  groups ( $>\text{SiOH}_w$ ).<sup>31</sup> Since the silica we used is mesoporous with a significant amount of internal porosity,<sup>35</sup> we interpret these  $>\text{SiOH}_w$  sites as silanols contained within internal pore spaces. The isolation of these species gives rise to the narrow line width of this peak. This peak is present in spectra of the control samples but significantly muted compared to the strong signal from surface water species. In the spectra collected for the Ni samples, the mobile water peak is entirely suppressed, unmasking the sharp peak from  $>\text{SiOH}_w$  and a peak peak at 5.5 ppm from strongly H-bonded  $>\text{SiOH}$  groups ( $>\text{SiOH}_s$ ).<sup>31</sup> This peak is also present as a shoulder in all other  $^1\text{H}$  spectra but difficult to resolve from the main  $\text{H}_2\text{O}$  peak. These  $>\text{SiOH}_s$  sites represent silanols on the external surface which are hydrogen bonded to the surface water species. The strong suppression of the water peaks indicates that these surface waters are strongly interacting with the paramagnetic cation species, and the  $>\text{SiOH}$  surface groups are largely unperturbed. The proton NMR provide complementary evidence that Ni and Cu sorb to the  $>\text{SiO}^-$  sites near surface water.

The measured  $^1\text{H}$  relaxation properties ( $T_1$ ) can be related to the relative proximity of the surface protonated species to the sorbed paramagnetic species and can be used to further constrain the structural models for the sorption process (Table 2). The results, again, indicate that the paramagnets are most

**Table 2.**  $^1\text{H}$  MAS NMR Results for the Sorption Samples

sample	site	chemical shift (ppm)	$T_1$ (ms)
control pH 9	$>\text{SiOH}_s$	5.82	$250 \pm 2$
	$\text{H}_2\text{O}$	4.74	$155 \pm 1$
	$>\text{SiOH}_w$	2.38	$581 \pm 15$
Cu 01	$>\text{SiOH}_s$	5.46	$140 \pm 1$
	$\text{H}_2\text{O}$	4.92	$89.2 \pm 0.1$
	$>\text{SiOH}_w$	2.38	$612 \pm 1$
Cu 1	$>\text{SiOH}_s$	5.54	$110 \pm 1$
	$\text{H}_2\text{O}$	4.56	$38.1 \pm 0.1$
	$>\text{SiOH}_w$	2.37	$317 \pm 1$
Ni 01	$>\text{SiOH}_s$	5.48	$105 \pm 1$
	$\text{H}_2\text{O}$	-	-
	$>\text{SiOH}_w$	2.38	$685 \pm 1$
Ni 1	$>\text{SiOH}_s$	5.48	$106 \pm 1$
	$\text{H}_2\text{O}$	-	-
	$>\text{SiOH}_w$	2.38	$564 \pm 1$

closely associated with sorbed surface water but do exert some influence on the  $>\text{SiOH}_s$  and  $>\text{SiOH}_w$  species. The observed  $^1\text{H}$   $T_1$  can be thought to contain contributions from two separate interactions through the relation

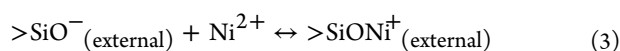
$$1/T_1 = 1/T_{1P} + 1/T_{1\text{dia}} \quad (1a)$$

where  $1/T_{1P}$  is the contribution from the paramagnetic species, and  $1/T_{1\text{dia}}$  is the contribution from all other diamagnetic interactions (e.g.,  $^1\text{H}$ - $^1\text{H}$  spin diffusion, and  $^1\text{H}$ - $^{29}\text{Si}$  dipole coupling).<sup>23</sup> The paramagnetic contribution here is proportional to the distance ( $r$ ) between  $^1\text{H}$  and the paramagnet center and the number of the paramagnetic species ( $N_p$ )<sup>36</sup>

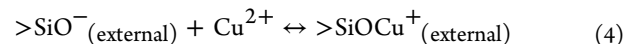
$$1/T_{1P} \propto N_p \cdot 1/r^6 \quad (2)$$

We use the above relationships only as guides for the discussion of the measured  $T_1$  values and how we can relate these to relative proximity of the paramagnet species. In general, we can state that the  $T_1$  of a  $^1\text{H}$  species will decrease if either the distance to the paramagnet decreases or the density of paramagnets increases. We note the most dramatic decreases of the  $T_1$  values relative to the control for the residual water peaks, followed by the  $>\text{SiOH}_s$  sites (Table 2). With the exception of the highest surface loading Cu sample, the  $T_1$  of the  $>\text{SiOH}_w$  is largely unaffected. These data indicate that in the Cu system, at the highest loadings, the paramagnet is in close enough proximity to affect the relaxation properties of the  $>\text{SiOH}_w$ . In all other samples, the paramagnet species are most closely associated with surface sorbed water and the strongly H-bonded silanol sites.

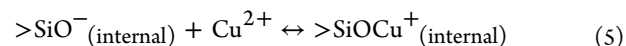
**Sorption Complexation Models.** We frame these results within the context of simple sorption models where the metals sorb to a single type of surface site. In the Ni system we propose that the sorption behavior observed can be explained by a single surface reaction



The  $^1\text{H}$  data indicate that the Ni does not interact with the internal silanol sites ( $>\text{SiOH}_w$ ) and that all the sorption reactions occur at the external surface sites. In the Cu system, the data suggests that a two stage sorption model is necessary to describe the  $^{29}\text{Si}\{^1\text{H}\}$  CP/MAS and  $^1\text{H}$  NMR data. At lower concentrations the Cu sorbs following the reaction



As these external sites become less favorable at higher surface coverages the Cu then sorbs at sites within the internal pore spaces via



This second step is evidenced by the shortening of the  $>\text{SiOH}_w$   $T_1$  as the Cu loading increases which indicates a closer association of the Cu with these internal sites. It is unclear why these same processes are not active in the Ni system. One possible explanation could be that diffusion of large Ni complexes to these internal sites is limited. More work is necessary to determine if these processes are active. In general, these results agree well with previous solution chemistry studies which predict the inner sphere sorption of Cu and Ni at the silica surface.<sup>3,37</sup> We believe that the NMR techniques presented here can be easily extended to probe a range of interactions between paramagnetic sorbates and diamagnetic surfaces. The results of such studies should help grow our understanding of the basic reactions needed to model the fate and transport of metals.

## AUTHOR INFORMATION

### Corresponding Author

\*E-mail: mason42@llnl.gov.

### Notes

The authors declare no competing financial interest.

## ACKNOWLEDGMENTS

This work was funded by the U.S. Department of Energy's Office of Science through Basic Energy Science Geosciences Division and the Subsurface Biogeochemical Research program within the Biological and Environmental Research, Climate and Environmental Sciences Division. This work was also performed under the auspices of the U.S. Department of Energy by Lawrence Livermore National Laboratory under Contract W-7405-Eng-48 and Contract DE-AC52-07NA27344

## REFERENCES

- (1) Davis, J. A.; James, R. O.; Leckie, J. O. Surface ionization and complexation at the oxide/water interface: I. Computation of electrical double layer properties in simple electrolytes. *J. Colloid Interface Sci.* **1978**, *63* (3), 480–499.
- (2) Dzombak, D. A.; Morel, F. o. M. M. *Surface complexation modeling: hydrous ferric oxide*; Wiley: New York, 1990; p xvii, 393 p.
- (3) Criscenti, L. J.; Sverjensky, D. A. The role of electrolyte anions ( $\text{ClO}_4^-$ ), ( $\text{NO}_3^-$ ), and ( $\text{Cl}^-$ ) in divalent metal ( $\text{M}(2+)$ ) adsorption on oxide and hydroxide surfaces in salt solutions. *Am. J. Sci.* **1999**, *299* (10), 828–899.
- (4) Sverjensky, D. A. Interpretation and prediction of triple-layer model capacitances and the structure of the oxide-electrolyte-water interface. *Geochim. Cosmochim. Acta* **2001**, *65* (21), 3643–3655.
- (5) Criscenti, L. J.; Sverjensky, D. A. A single-site model for divalent transition and heavy metal adsorption over a range of metal concentrations. *J. Colloid Interface Sci.* **2002**, *253* (2), 329–352.

- (6) Karamalidis, A. K.; Dzombak, D. A. *Surface complexation modeling: gibbsite*; Wiley: Hoboken, NJ, 2010; p xv, 294 p.
- (7) Xia, K.; Mehadi, A.; Taylor, R. W.; Bleam, W. F. X-ray absorption and electron paramagnetic resonance studies of Cu(II) sorbed to silica: Surface-induced precipitation at low surface coverages. *J. Colloid Interface Sci.* **1997**, *185* (1), 252–257.
- (8) Xia, K.; Taylor, R. W.; Bleam, W. F.; Helmke, P. A. The distribution of Cu(II) on boehmite and silica surfaces: Correlating EPR signal loss with the effective Bohr magneton number of sorbed ions. *J. Colloid Interface Sci.* **1998**, *199* (1), 77–82.
- (9) Cheah, S. F.; Brown, G. E.; Parks, G. A. XAFS spectroscopy study of Cu(II) sorption on amorphous SiO<sub>2</sub> and gamma-Al<sub>2</sub>O<sub>3</sub>: Effect of substrate and time on sorption complexes. *J. Colloid Interface Sci.* **1998**, *208* (1), 110–128.
- (10) Cheah, S. F.; Brown, G. E.; Parks, G. A. XAFS study of Cu model compounds and Cu<sup>2+</sup> sorption products on amorphous SiO<sub>2</sub>, gamma-Al<sub>2</sub>O<sub>3</sub>, and anatase. *Am. Mineral.* **2000**, *85* (1), 118–132.
- (11) Motschi, H. Correlation of EPR-parameters with thermodynamic stability constants for copper(II) complexes Cu(II)-EPR as a probe for the surface complexation at the water/oxide interface. *Colloids Surf.* **1984**, *9* (4), 333–347.
- (12) Hyun, S. P.; Cho, Y. H.; Hahn, P. S. An electron paramagnetic resonance study of Cu(II) sorbed on quartz. *J. Colloid Interface Sci.* **2003**, *257* (2), 179–187.
- (13) Roberts, D. R.; Scheidegger, A. M.; Sparks, D. L. Kinetics of Mixed Ni–Al Precipitate Formation on a Soil Clay Fraction. *Environ. Sci. Technol.* **1999**, *33* (21), 3749–3754.
- (14) Scheinost, A. C.; Ford, R. G.; Sparks, D. L. The role of Al in the formation of secondary Ni precipitates on pyrophyllite, gibbsite, talc, and amorphous silica: a DRS study. *Geochim. Cosmochim. Acta* **1999**, *63* (19–20), 3193–3203.
- (15) Scheinost, A. C.; Sparks, D. L. Formation of Layered Single- and Double-Metal Hydroxide Precipitates at the Mineral/Water Interface: A Multiple-Scattering XAFS Analysis. *J. Colloid Interface Sci.* **2000**, *223* (2), 167–178.
- (16) Sheng, G.; Yang, S.; Sheng, J.; Hu, J.; Tan, X.; Wang, X. Macroscopic and Microscopic Investigation of Ni(II) Sequestration on Diatomite by Batch, XPS, and EXAFS Techniques. *Environ. Sci. Technol.* **2011**, *45* (18), 7718–7726.
- (17) Carroll, S. A.; Maxwell, R. S.; Bourcier, W.; Martin, S.; Hulsey, S. Evaluation of silica-water surface chemistry using NMR spectroscopy. *Geochim. Cosmochim. Acta* **2002**, *66* (6), 913–926.
- (18) Houston, J. R.; Herberg, J. L.; Maxwell, R. S.; Carroll, S. A. Association of dissolved aluminum with silica: Connecting molecular structure to surface reactivity using NMR. *Geochim. Cosmochim. Acta* **2008**, *72* (14), 3326–3337.
- (19) Kim, Y.; Kirkpatrick, R. J. Na-23 and Cs-133 NMR study of cation adsorption on mineral surfaces: Local environments, dynamics, and effects of mixed cations. *Geochim. Cosmochim. Acta* **1997**, *61* (24), 5199–5208.
- (20) Li, W.; Feng, J.; Kwon, K. D.; Kubicki, J. D.; Phillips, B. L. Surface Speciation of Phosphate on Boehmite (gamma-AlOOH) Determined from NMR Spectroscopy. *Langmuir* **2010**, *26* (7), 4753–4761.
- (21) Mason, H. E.; Maxwell, R. S.; Carroll, S. A. The formation of metastable aluminosilicates in the Al–Si–H<sub>2</sub>O system: Results from solution chemistry and solid-state NMR spectroscopy. *Geochim. Cosmochim. Acta* **2011**, *75* (20), 6080–6093.
- (22) Wickramasinghe, N. P.; Ishii, Y. Sensitivity enhancement, assignment, and distance measurement in <sup>13</sup>C solid-state NMR spectroscopy for paramagnetic systems under fast magic angle spinning. *J. Magn. Reson.* **2006**, *181* (2), 233–243.
- (23) Wickramasinghe, N. P.; Shaibat, M. A.; Ishii, Y. Elucidating connectivity and metal-binding structures of unlabeled paramagnetic complexes by C-13 and H-1 solid-state NMR under fast magic angle spinning. *J. Phys. Chem. B* **2007**, *111* (33), 9693–9696.
- (24) Clark, D. L.; Hobart, D. E.; Palmer, P. D.; Sullivan, J. C.; Stout, B. E. <sup>13</sup>C NMR characterization of actinyl(VI) carbonate complexes in aqueous-solution. *J. Alloys Compd.* **1993**, *193* (1–2), 94–97.
- (25) Cordella, C. Principal component analysis: the basic building block of chemometrics. *Actual. Chim.* **2010**, *345*, 13–18.
- (26) Ayoko, G. A.; Mostert, M. M. R.; Kokot, S. Application of chemometrics to analysis of soil pollutants. *TrAC, Trends Anal. Chem.* **2010**, *29* (5), 430–445.
- (27) Hasegawa, T. Chemometrics for spectroscopic analysis. *Anal. Bioanal. Chem.* **2003**, *375* (1), 18–19.
- (28) Maeder, M. Evolving factor analysis for the resolution of overlapping chromatographic peaks. *Anal. Chem.* **1987**, *59* (3), 527–530.
- (29) de Juan, A.; Tauler, R. Chemometrics applied to unravel multicomponent processes and mixtures - Revisiting latest trends in multivariate resolution. *Anal. Chim. Acta* **2003**, *500* (1–2), 195–210.
- (30) Tauler, R. Multivariate curve resolution applied to second order data. *Chemom. Intell. Lab.* **1995**, *30* (1), 133–146.
- (31) Liu, C. H. C.; Maciel, G. E. The fumed silica surface: A study by NMR. *J. Am. Chem. Soc.* **1996**, *118* (21), 5103–5119.
- (32) Kolodziejski, W.; Klinowski, J. Kinetics of cross-polarization in solid-state NMR: A guide for chemists. *Chem. Rev.* **2002**, *102* (3), 613–628.
- (33) Crank, J. *The mathematics of diffusion*; Clarendon Press: Oxford, 1956; p 347.
- (34) Goldman, M.; Shen, L. Spin-spin relaxation in LAF3. *Phys. Rev.* **1966**, *144* (1), 321–8.
- (35) Loucaides, S.; Behrends, T.; Van Cappellen, P. Reactivity of biogenic silica: Surface versus bulk charge density. *Geochim. Cosmochim. Acta* **2010**, *74* (2), 517–530.
- (36) Voronov, V. K.; Keiko, V. V.; Moskovskaya, T. E. Paramagnetic reagents for the study of the structure of heteroatomic compounds from the NMR spectra. *J. Struct. Chem.* **1977**, *18*, 5.
- (37) Vlasova, N. N. Adsorption of Cu<sup>2+</sup> ions onto silica surface from aqueous solutions containing organic substances. *Colloids Surf., A* **2000**, *163* (2–3), 125–133.